

1 **Response to “Comment to “*The transition on North America from the***
2 ***warm humid Pliocene to the glaciated Quaternary traced by eolian dust***
3 ***deposition at a benchmark North Atlantic Ocean drill site, by David***
4 ***Lang et al. Quaternary Science Reviews 93: 125-141””***

5 David C. Lang¹, Ian Bailey², Paul A. Wilson¹, Gavin L. Foster¹, Clara T. Bolton³,

6 Oliver Friedrich⁴, Marcus Gutjahr⁵

7 ¹National Oceanography Centre Southampton, University of Southampton, Waterfront Campus,
8 European Way, Southampton SO14 3ZH, UK.

9 ²Camborne School of Mines, College of Engineering, Mathematics & Physical Sciences, University of
10 Exeter, Penryn Campus, Treliiever Road, Penryn, Cornwall TR10 9FE, UK.

11 ³Facultad de Geología, Universidad de Oviedo, Campus de Llamaquique, Jesús Arias, de Velasco s/n,
12 33005 Oviedo, Spain.

13 ⁴Institute of Earth Sciences, University of Heidelberg, Im Neuenheimer Feld 234-236, 69120
14 Heidelberg, Germany.

15 ⁵GEOMAR Helmholtz Centre for Ocean Research Kiel, Wischhofstrasse 1-3, 24148 Kiel, Germany.

16

17 **1. Introduction**

18 In volume 93 of Quaternary Science Reviews we published a new record of
19 terrigenous inputs to Integrated Ocean Drilling Program (IODP) Site U1313 that
20 tracks the history of aeolian dust deposition in the North Atlantic Ocean and aridity on
21 North America during the late Pliocene-earliest Pleistocene intensification of northern
22 hemisphere glaciation (iNHG, 3.3 to 2.4 Ma). Naafs et al. (2014) are generally
23 supportive but question one of our conclusions, specifically our argument that
24 “*glacial grinding and transport of fine grained sediments to mid latitude outwash*
25 *plains is not the fundamental mechanism controlling the magnitude of the flux of*
26 *higher plant leaf waxes from North America to Site U1313 during iNHG.*” They
27 suggest that our argument “is predominantly based on our observation that the

28 relationship between sediment lightness (L^*)-based terrigenous inputs and dust-
29 derived biomarkers, which is observed to be linear elsewhere (Martínez-Garcia et al.,
30 2011), is non-linear at Site U1313.”

31 We welcome their interest and the opportunity to clarify one or two
32 misunderstandings. Contrary to their impression, our argument that the role of glacial
33 grinding is not the principle driver of increased North American aeolian dust flux to
34 the mid latitude North Atlantic during iNHG is based mainly on our radiogenic
35 isotope provenance data (not on the non-linear relationship between biomarker and
36 terrigenous dust inputs). Our provenance data indicate a North American source for
37 this dust (~3.3 to 2.4 Ma) in keeping with the interpretation of the biomarker data.
38 Crucially, however, all of our data point to a mid-latitude provenance regardless of
39 (inter)glacial state. This finding is inconsistent with the Naafs et al. (2012; 2014)
40 interpretation of the importance of glacial grinding and transport to mid latitude
41 outwash plains for deflation because of the radically changing latitudinal extent of
42 continental ice on North America throughout this this 900 kyr-long interval.
43 Nevertheless, below we critically reassess this ‘non-linearity’ issue in light of Naafs et
44 al. (2014) making available some of the XRF data from Site U1313 and then explain
45 why the evidence presented in Lang et al. (2014) supports our original conclusions.

46

47 **2. Non-linearity between dust biomarkers and terrigenous inputs at Site U1313.**

48 As highlighted in Lang et al. (2014), our desire to generate an orbital-resolution
49 record of terrigenous inputs to Site U1313 by calibrating a high resolution record of
50 L^* with discrete measurements of percent calcium carbonate (%CaCO₃) was driven
51 by: 1) the pioneering work on Deep Sea Drilling Project Site 607 on the observed
52 relationship between variations in %CaCO₃ and Neogene climate (Ruddiman et al.,

53 1987) and 2) observations of the IODP Expedition 306 Scientists (2006), specifically
54 those of Jens Grützner who correlated variations in L* at Site U1313 to the LR04
55 global benthic $\delta^{18}\text{O}$ stack for the past 3.3 Ma on board the JOIDES *Resolution*, during
56 IODP Exp. 306 (an expedition in which one of us (IB) participated and contributed to
57 the team effort to generate this remarkable sediment colour record).

58 Having demonstrated that variations in %CaCO₃ at Site U1313 are not driven
59 by dissolution (as originally hypothesized by Ruddiman et al., 1989), Lang et al.
60 (2014) used the relationship found between discrete measurements of %CaCO₃ and
61 the higher resolution shipboard L* record (Fig. 3 of Lang et al. (2014)) to generate a
62 proxy record of terrigenous inputs in the interval for which a high quality independent
63 age model exists (3.3 to 2.4 Ma, Bolton et al. (2010)). Naafs et al. (2014) suggest that
64 this L*-derived record of terrigenous inputs is “biased” for two reasons: (i) because
65 our choice of a linear calibration equation results in an overestimation of %CaCO₃
66 from the L* record and therefore an underestimation of terrigenous content for key
67 glacials such as marine isotope stage (MIS) 100 (2.52 Ma) and, (ii) because the non-
68 carbonate fraction at Site U1313 does not only reflect variations in aeolian dust inputs.
69 Instead, they use a scanning XRF-derived record of elemental Fe intensity data to re-
70 assess the relationship between dust biomarker and terrigenous inputs asserting that
71 the XRF record represents “a pure terrigenous signal in the absence of a large input of
72 ice-raftered debris (IRD).”

73 Both the L*-to-CaCO₃ and XRF-Fe count datasets, used as proxies for aeolian
74 dust, are subject to the same potential sources of ‘contamination’ (e.g., from
75 diagenetically derived iron sulphides, volcanic ash or IRD in the clay through sand-
76 sized sediment fractions). As originally noted in Lang et al. (2014), factors in addition
77 to variations in CaCO₃ content can lead to changes in L* (Balsam et al. 1999) and

78 similar issues arise with the use of XRF records. Specifically we caution against use
79 of XRF elemental intensity data that are either not converted to dimensionless units or
80 to percent Fe data. The absolute values of XRF-derived elemental intensity data can
81 be strongly influenced by sediment inhomogeneity (e.g., variations in sediment water
82 content, grain-size distribution and irregularities in the split core surface) (Weltje and
83 Tjallingii, 2008). We would welcome publication of data series of the natural
84 logarithms of Fe/Ca and Ti/Ca derived from the XRF data that were obtained when
85 the Site U1313 cores were scanned because a log-ratio calibration model provides a
86 more reliable prediction of sediment element concentrations from XRF core-scanner
87 output than that derived from elemental intensities alone (Weltje and Tjallingii, 2008).

88 Regardless, it is perhaps useful to re-emphasize an observation that we
89 stressed in Lang et al. (2014): Non-linearity in the relation between the biomarker
90 record and our terrigenous record cannot be explained by ‘contamination’ of the
91 terrigenous fraction at Site U1313 by contributions invoked from sources other than
92 dust (e.g. from IRD and volcanism as documented for MIS 100 by Bolton et al., 2010).
93 This is because additional terrigenous inputs would act to amplify the terrigenous
94 rather than the biomarker record during glaciations and IRD and volcanic
95 accumulation rates are always higher in glacials than in interglacials. Thus, there is no
96 way to explain amplification of the glacial values in the biomarker record (relative to
97 the terrigenous fraction) by invoking decreases in IRD and/or volcanic inputs while a
98 linear relation is maintained between biomarker and lithogenic dust. In other words,
99 some mechanism (increased export/burial efficiency of biomarkers or vegetation
100 biome shifts) must act to amplify the glacial jumps in the biomarker record relative to
101 those in the terrigenous record.

102

103 Naafs et al. (2014) raise concern over the fact that the linear equation used by
104 Lang et al. (2014) to produce a high resolution record of %CaCO₃ from the Site
105 U1313 L* record underestimates the abundance of the terrigenous sedimentary
106 component (%terrigenous) deposited at this site during MIS 100 by up to 6.8%. MIS
107 100 is a key glacial in this context because Lang et al. (2014) suggest that it is
108 characterised by one of the most pronounced amplifications of biomarker content
109 relative to terrigenous content during iNHG. We agree that it is not possible to
110 determine via regression analysis whether a cross plot of %terrigenous (derived from
111 our discrete CaCO₃ data) and biomarker abundance for our iNHG study interval
112 exhibits non-linearity. But the question is whether or not we see non-linearity or
113 amplification in the contribution of biomarkers to terrigenous content at Site U1313
114 *during certain glacials* (rather than for the full population of discrete %terrigenous
115 data, n = 119 over ~5.3-2.4 Ma) and that question is not best addressed by simple
116 cross plots. This is why we sought to assess the evolution of non-linearity between
117 these two parameters in the time series presented in Fig. 10 of Lang et al. (2014).
118 Ratios of *n*-alkane abundance to the fractional percentage of the terrigenous
119 component from Site U1313 (i.e. nannograms of biomarkers per gram of terrigenous
120 sediment), with full error propagation, derived from our original
121 discrete %terrigenous dataset and from a new higher resolution record of CaCO₃ for
122 MIS G7-99 (n = 102, every 10 cm) from the secondary splice (118.65-130.8 mcd)
123 show that amplification of biomarker inputs relative to terrigenous deposition (i.e., a
124 non-linear relationship) is real for MIS 100 and other big glacials from 2.7 Ma
125 onwards (Fig. 1). In fact, a similar result is also obtained for iNHG in the time domain
126 when the biomarker data are compared to the XRF-derived Fe (albeit elemental
127 intensity) data of Naafs et al. (2014).

128

129 **3. The importance of non-glaciogenic versus glacial grinding mechanisms of dust**
130 **generation for terrigenous deposition at Site U1313 during iNHG**

131 Naafs et al. (2012; 2014) argue that the sharp increase in the deposition of aeolian
132 dust biomarkers at Site U1313 from 2.72 Ma is related to an increase in the
133 availability of dust for deflation on North America due to expansion of glacial
134 outwash plains south of a North American Ice Sheet during MIS G6. This mechanism
135 was plausible based on the evidence available to Naafs et al. (2012) but, as explained
136 in Lang et al. (2014), it is inconsistent with the uniformly mid latitude provenance of
137 the terrigenous material at Site U1313 throughout iNHG (regardless of glacial-
138 interglacial state) and the failure of North American ice sheets to advance into the
139 mid-latitudes by G6 (and probably not until MIS 100, Fig. 2).

140 In Lang et al. (2014) we noted that, in the absence of significant NHG prior to
141 MIS G6 (Kleiven et al., 2002), the large fluxes that we observe for terrigenous
142 deposition at Site U1313 prior to 2.7 Ma indicate that non-glaciogenic mechanisms of
143 aeolian dust generation represent important sources of terrigenous sediment for our
144 study site. We also demonstrated that the terrigenous component deposited at Site
145 U1313 throughout iNHG has a definitive (non-volcanic) mid-latitude origin
146 independent of (inter)glacial state and, critically, that the provenance of this sediment
147 does not change across the onset of significant NHG, ~2.7 Ma. These observations
148 suggest that the dominant sources of dust deposited at our study site, and the
149 mechanisms responsible for its generation on North America, remained unchanged
150 across 2.7 Ma despite the big glacial increases in both the L*- and biomarker-derived
151 records of dust accumulation at Site U1313 across this interval.

152 Our provenance data show that if glacial outwash plains on North America
153 were the dominant source of aeolian dust deposited at Site U1313 from ~2.7 Ma, a
154 large proportion of the subglacial erosion responsible for generating this material
155 would have been required to take place in the mid latitudes of North America¹. Yet,
156 this requirement is at odds with important lines of evidence (including one of those
157 used by Naafs et al. (2014)). Comparison of the history of biomarker accumulation at
158 Site U1313 with the reconstructions of glacial extent on North America from
159 observation-constrained inverse ice-ocean modelling (de Boer et al., 2014) (Fig. 2)
160 and diverse geological lines of evidence (Brigham-Grette et al., 2013; Balco and
161 Rovey, 2010; Bailey et al., 2013; Hennissen et al., 2014) indicates that, although late
162 Pleistocene-magnitude glacial fluxes in biomarkers are established at Site U1313
163 during MIS G6, glacial expansion on North America around 2.7 Ma was modest (Fig.
164 2). Results from the inverse ice-ocean modeling reconstruct small (~12 of sea-level
165 equivalent ice volume) ice caps restricted to Alaska and the high latitudes of Canada
166 (mainly centred on Hudson Bay;
167 http://www.staff.science.uu.nl/~boer0160/data_anice_5myr/) where they would have
168 been emplaced on predominantly Archaean bedrock having a much more extreme
169 unradiogenic isotope composition than the terrestrial material accumulating at Site
170 U1313 (Lang et al., 2014). These observations raise a serious question mark over the
171 plausibility of glacial grinding as the mechanism responsible for the order of
172 magnitude increase in biomarker deposition ~2.7 Ma.

173

174 **4. Conclusions**

¹As was the case for the Last Glacial, which is why North American terrestrial loess deposits are isotopically similar to the signature of mid-latitude North American geologic terranes (Aleinikoff et al., 1999; Lang et al., 2014).

175 In keeping with the previous work of three of us (IB, GLF, PAW, e.g., Bailey et al.
176 (2013)), we did not suggest in Lang et al. (2014) that North America remained
177 unglaciated during MIS G6, 2.7 Ma. We maintain, however, that the indirect impact
178 of ice-sheet growth on aridity, vegetation and westerly wind strength south of the
179 North American ice sheet (the “non-glaciogenic” mechanisms) played a far greater
180 role in controlling the magnitude of North America dust delivery to the mid latitude
181 North Atlantic Ocean during iNHG than the direct contribution of glacial grinding.

182

183 **5. Acknowledgements**

184 We thank David Naafs for making available the secondary splice XRF Fe data for Site
185 U1313 and David Hodell for access, at short notice, to his LECO carbon analyser at
186 the Godwin Laboratory, Cambridge University to permit generation of additional
187 CaCO₃ data from the secondary splice at Site U1313 (data available on the on-line
188 Pangaea database).

189

190 **6. References**

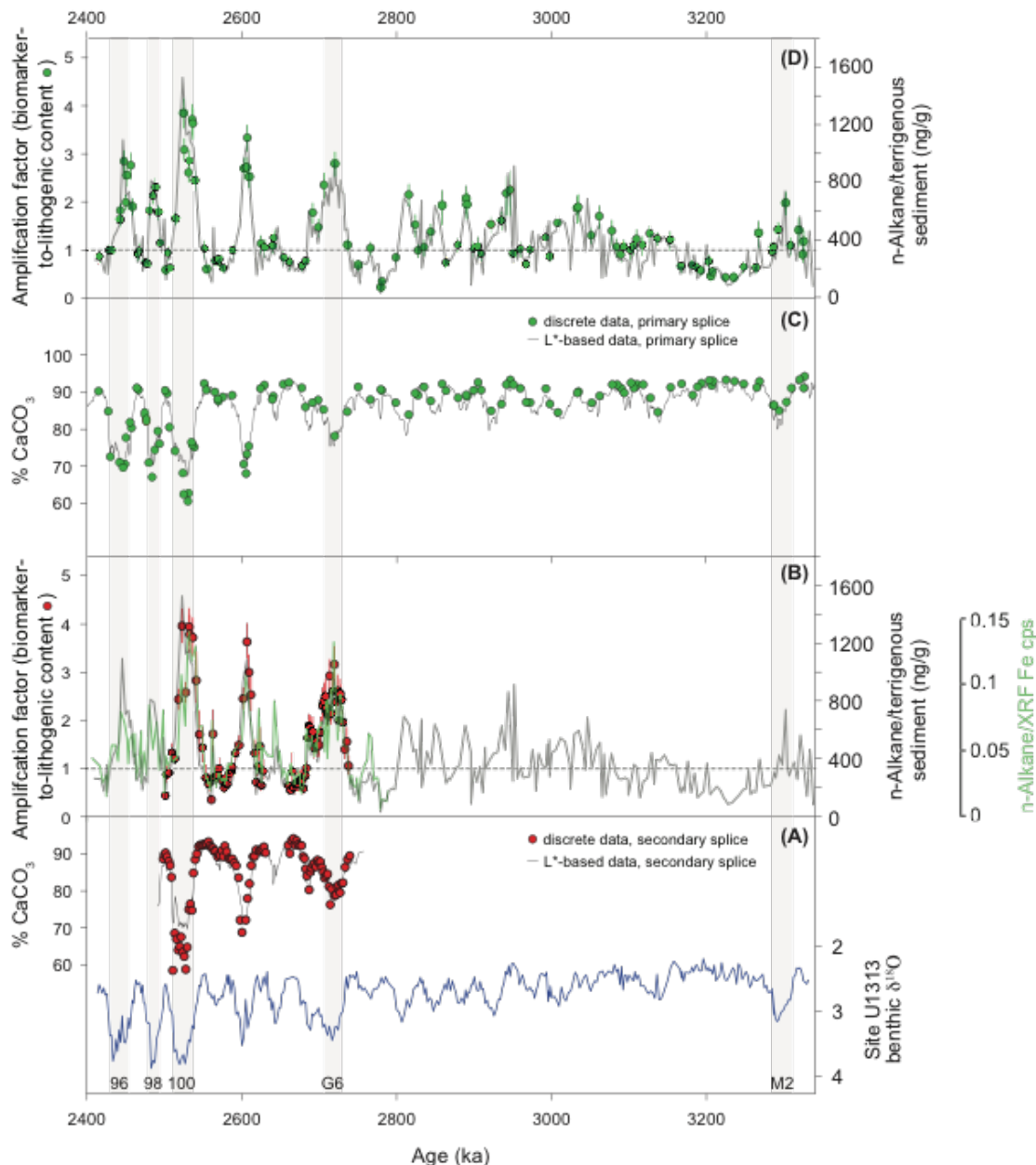
- 191 Aleinikoff, J.N., Muhs, D.R., Sauer, R.R., Fanning, C.M., 1999. Late Quaternary
192 loess in northeastern Colorado, II–Pb isotopic evidence for the variability of
193 loess sources. Geol. Soc. Am. Bull. 111, 1876–1883.
- 194 Bailey, I., Hole, G.M., Foster, G.L., Wilson, P.A., Storey, C.D., Trueman, C.N.,
195 Raymo, M.E., 2013. An alternative suggestion for the Pliocene onset of major
196 northern hemisphere glaciation based on the geochemical provenance of North
197 Atlantic Ocean ice rafted debris. Quaternary Science Reviews 75 (1), 181–
198 194, doi: 10.1016/j.quascirev.2013.06.004.
- 199 Balco, G., Rovey II, C.W., 2010. Absolute chronology for major Pleistocene advances

- 200 of the Laurentide Ice Sheet. *Geology* 38, 795–798.
- 201 Balsam, W.L., Deaton, B.C., Damuth, J.E., 1999. Evaluating optical lightness as a
202 proxy for carbonate content in marine sediment cores. *Marine Geology* 161
203 (2–4), 141-153. doi:10.1016/S0025-3227(99)00037-7.
- 204 Bolton, C.T., Wilson, P.A., Bailey, I., Friedrich, O., Beer, C.J., Becker, J., Baranwal,
205 S., et al., 2010. Millennial-scale climate variability in the subpolar North
206 Atlantic Ocean during the late Pliocene. *Paleoceanography* 25 PA4218, doi:
207 10.1029/2010PA001951.
- 208 Brigham-Grette, J., et al., 2013. Pliocene warmth, polar amplification, and stepped
209 pleistocene cooling recorded in NE arctic Russia. *Science* 340 (6139), 1421–
210 1427. <http://dx.doi.org/10.1126/science.1233137>.
- 211 de Boer, B., Lourens, L.J., van de Wal., R.S.W., 2014. Persistent 400,000-year
212 variability of Antarctic ice volume and the carbon cycle is revealed
213 throughout the Plio-Pleistocene. *Nature Communications* 5:2999,
214 doi:10.1038/ncomms3999.
- 215 Expedition 306 Scientists, 2006. Site 1313, in North Atlantic climate. *Proc. Integr.*
216 *Ocean. Drill. Program* 303/306. <http://dx.doi.org/10.2204/iodp.proc.303306.112.2006>.
- 217 Hennissen, J.A.I., Head, M.J., De Schepper, S., Groeneveld, J., 2014. Palynological
218 evidence for a southward shift of the North Atlantic Current at ~2.6 Ma during
219 the intensification of late Cenozoic Northern Hemisphere glaciation.
220 *Paleoceanography* 29(6), 564–580, doi:10.1002/2013PA002543
- 221 Kleivene, F.,H., Jansen, E., Fronval, T., Smith, T.M., 2002. Intensification of

- 223 Northern hemisphere glaciations in the circum Atlantic region (3.5–2.4 Ma) -
224 ice rafted detritus evidence. *Palaeogeogr. Palaeoclimatol. Palaeoecol.* 184,
225 213–223.
- 226 Lang, D.C., Bailey, I., Wilson, P.A., Beer, C.J., Bolton, C.T., Friedrich, O.,
227 Newsam, C., et al., 2014. The transition on North America from the warm
228 humid Pliocene to the glaciated Quaternary traced by eolian dust deposition at
229 a benchmark North Atlantic Ocean drill site. *Quaternary Science Reviews* 93
230 125–141, doi: 10.1016/j.quascirev.2014.04.005.
- 231 Lisiecki, L.E., Raymo, M.E., 2005. A PliocenePleistocene stack of 57 globally
232 distributed benthic $\delta^{18}\text{O}$ records. *Paleoceanog* 20, PA1003. <http://dx.doi.org/10.1029/2004PA001071>.
- 233 Martínez-Garcia, A., Rosell-Melé, A., Jaccard, S.L., Geibert, W., Sigman, D.M., et
234 al., 2011. Southern Ocean dustclimate coupling over the past four million
235 years. *Nature* 476, 312–315. <http://dx.doi.org/10.1038/nature10310>.
- 236 Naafs, B.D.A., Hefter, J., Acton, G., Haug, G.H., Martínez-Garcia, A., Pancost, R.,
237 Stein, R., 2012. Strengthening of North American dust sources during the late
238 Pliocene (2.7 Ma). *Earth and Planetary Science Letters* 317-318, 8–19. doi:
239 [10.1016/j.epsl.2011.11.026](http://dx.doi.org/10.1016/j.epsl.2011.11.026).
- 240 Naafs, B.D.A, Martínez-Garcia, A., Grützner, J., Higgins, S., 2014. Comment to “*The
241 transition on North America from the warm humid Pliocene to the glaciated
242 Quaternary traced by eolian dust deposition at a benchmark North Atlantic
243 Ocean drill site*, by David Lang et al. *Quaternary Science Reviews* 93: 125-
244 141” *Quaternary Science Reviews*.
- 245 Ruddiman, W.F., McIntyre, A., Raymo, M.E., 1987. Paleoenvironmental results from
246 North Atlantic sites 607 and 609. *Initial. Rep. DSDP* 94, 855–878.

248 Weltje, G.J., Tjallingii, R., 2008. Calibration of XRF core scanners for quantitative
249 geochemical logging of sediment cores: Theory and application. *Earth and*
250 *Planetary Science Letters* 274, 423–438, doi:10.1016/j.epsl.2008.07.054.

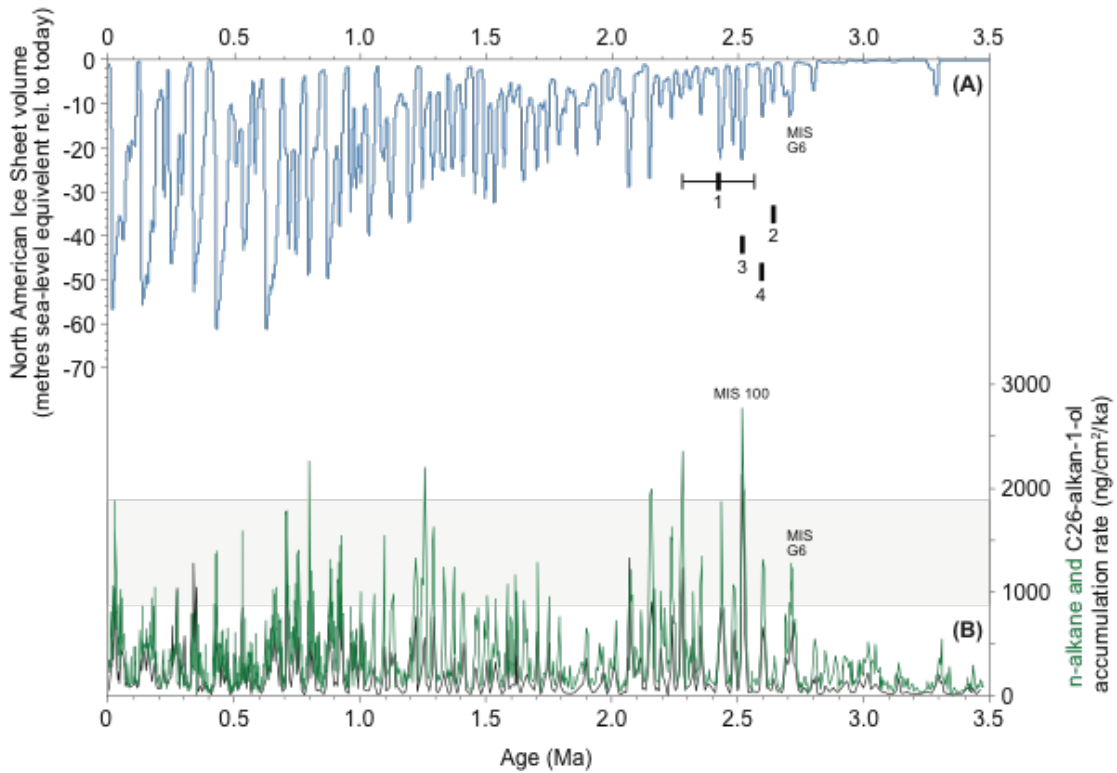
251 7. Figure captions



252

253 Fig. 1. New (this study) and published data sets (Lang et al., 2014 and Naafs et al., 2012) from IODP
254 Site U1313. Estimates of %CaCO₃ (**A & C**) and the ratio of the abundance of the long-chain odd *n*-
255 alkane (Naafs et al., 2012) and the terrigenous sediment component in Site U1313 sediments (**B & D**).
256 Also shown is time series of ratio of the abundance of n-alkanes (from primary splice) and XRF Fe
257 counts per second, cps, (from secondary splice; Naafs et al. (2014)) after converting secondary splice
258 composite depths assigned to the XRF Fe data to primary splice composite depths. Grey time series of
259 %CaCO₃ in **A & C** derived from sediment lightness (L*) data from the Site U1313 primary splice
260 estimated using a linear equation from Lang et al. (2014). Red %CaCO₃ data in **A** is new (this study).

261 Green %CaCO₃ data in C is from Lang et al. (2014). Terrigenous abundance data used to generate ratio
262 time series in B & D estimated using inverse fractional percentage (i.e. grams of terrigenous sediment
263 per gram of bulk sediment) of the L*-based proxy record of %CaCO₃ shown in A and C and of discrete
264 measurements of %CaCO₃ from both the secondary and primary splices also shown in A and C.
265 Vertical bars centred on red and green data in B & D represent propagated error (95% confidence
266 interval) based on individual external uncertainties reported for the discrete %CaCO₃ (based on
267 replicate measurements of a pure carbonate standard (± 1.4 wt.% (Lang et al., 2014), and ± 1.9 wt.%,
268 this study) and *n*-alkane measurements (7%, Martinez-Garcia et al., 2011). Amplification factors
269 shown in B & D represent normalisation of n-alkane/discrete %terrigenous ratio data by average ratio
270 for the Piacenzian PRISM time-slab (defined as 3.025–3.264 Ma) in our primary splice discrete
271 %terrigenous-derived ratio dataset. For consistency with Naafs et al. (2014) we linearly interpolate data
272 for the higher resolution records of the two datasets used to calculate the ratios shown in B & D so that
273 they match the resolution and specific ages of the data from the lower resolution records used. In B the
274 lower resolution record used to calculate all three ratio time series shown is the n-alkane abundance
275 data. Prior to assigning ages to our new %terrigenous data from the secondary splice (red data points in
276 A) the composite depths assigned to this record were converted to primary splice depths by manual
277 graphical correlation of Site U1313 primary and secondary splice L* records (tie points available on
278 Pangaea online database). For reference, also shown in A is Site U1313 benthic foraminiferal calcite
279 $\delta^{18}\text{O}$ data (Bolton et al., 2010). Vertical grey bars and labels denote key marine isotope stages. All data
280 plotted on the age model of Bolton et al. (2010).



281

282 Fig. 2. Relationship between simulated North American Ice Sheet extent (de Boer et al., 2014) (A) and
 283 dust biomarker deposition at Site U1313 (B) (Naafs et al., 2012) for the past 3.5 Myr shows that,
 284 although late Pleistocene-magnitude glacial fluxes in dust biomarkers are established at Site U1313
 285 during MIS G6, glacial expansion on North America around 2.7 Ma was modest and did not extend
 286 into the mid latitudes at this time. Horizontal grey bar in B denotes range of n-alkane accumulation
 287 rates associated with large-magnitude North American glacial episodes of the past ~700 kyr. 1 = timing
 288 of oldest evidence for mid-latitude glaciation of North America in the form of cosmogenic-nuclide
 289 dated glacial tills at 39°N in Missouri, USA at 2.41 ± 0.14 Ma (Balco and Rovey, 2010). 2 = Onset of
 290 North American-sourced IRD deposition in the open North Atlantic Ocean (Bailey et al., 2013). 3 =
 291 First time that Arctic air temperatures tend towards Last Glacial Maximum values (Brigham-Grette et
 292 al., 2013). 4 = First excursion of the polar front in the glacial North Atlantic Ocean south of ~53°N
 293 (Hennissen et al., 2014). MIS = marine isotope stages. All data plotted on published age models
 294 derived from the LR04 global benthic stack.